

# An Evaluation of the Hybrid Sparse/Diffuse Algorithm for Underwater Acoustic Channel Estimation

Nicolò Michelusi\*, Beatrice Tomasi\*, Urbashi Mitra<sup>†</sup>, James Preisig<sup>‡</sup>, and Michele Zorzi\*

\*Department of Information Engineering — University of Padova, Italy

<sup>†</sup>Ming Hsieh Department of Electrical Engineering — University of Southern California, (CA) USA

<sup>‡</sup>Department of Applied Ocean Physics and Engineering — Woods Hole Oceanographic Institution, (MA) USA

Email: michelusi@dei.unipd.it, tomasibe@dei.unipd.it, ubli@usc.edu, jpreisig@whoi.edu, zorzi@dei.unipd.it

**Abstract**—The underwater acoustic channel has been usually modeled as sparse. However, in some scenarios of interest, *e.g.*, shallow water environments due to the interaction with the surface and the seabed, the channel exhibits also a *dense* arrival of multipath components. In these cases, a Hybrid Sparse/Diffuse (HSD) channel representation, rather than a purely sparse one, may be more appropriate.

In this work, we present the HSD channel model and channel estimators based on it. We evaluate these estimation strategies on the SPACE08 experimental data set. We show that the HSD estimators outperform the more conventional purely sparse and least squares estimators. Moreover, we show that an exponential Power Delay Profile (PDP) for the diffuse component is appropriate in scenarios where the receiver is far away from the transmitter. Finally, the HSD estimators and the exponential PDP model are shown to be robust even in scenarios where the channel does not exhibit a diffuse component.

## I. INTRODUCTION

UnderWater Acoustic (UWA) communication is emerging as a technology for applications such as environmental monitoring, marine surveillance and ocean exploration [1], [2].

UWA channels exhibit challenging characteristics such as high attenuation, large channel delay spread, Doppler spread [3], [4] and, consequently, incur low throughput and reliability [5], relative to wireless terrestrial radiofrequency channels. In particular, the large delay spread causes intersymbol interference (ISI), which can be compensated by equalization of the received sequence. However, the performance of coherent equalizers is highly sensitive to the availability of accurate channel estimates. To this end, it is crucial to develop channel estimation strategies that exploit the intrinsic nature of UWA propagation to improve the estimation accuracy.

Due to the large inter-arrival delays of multipath components, relative to the delay resolution at the receiver, the UWA channel can be represented by sparse specular

arrivals that can be predicted by geometrically based ray-tracing algorithms, such as Bellhop [6], once the environmental conditions are known. For this reason, several UWA channel estimators based on *sparse approximations* and *compressed sensing* have been proposed and successfully employed in the literature [7]–[10]. In [11], a comparative study among purely sparse and Least Squares (LS) channel estimators has been performed, showing that the former, while improving the estimation accuracy when the channel is truly sparse, are robust even when the channel does not exhibit a sparse nature.

However, in many scenarios of interest in UWA communications, *e.g.*, shallow water environments, where the reflections of the sound waves from the seabed and sea surface give rise to a richer interaction among multipath components, also a dense UWA channel has been observed. For these scenarios, a purely sparse model does not appropriately represent the channel behavior. In [12] it is shown that shallow-water propagation channels exhibit high variability, ranging from stable single-path propagation to overspread, and from sparse to densely populated impulse responses. This is caused by the rough surface scattering and by inhomogeneities in the water column, which induce different angles of arrival of the multipath components that superimpose at the receiver according to constructive and destructive interference patterns.

Although robust [11], channel estimators based on the assumption of a purely sparse channel are not expected to perform well when the channel is not purely sparse. For this reason, it is crucial to design channel estimation strategies attaining high accuracy even in the scenarios where the channel exhibits a dense, or a hybrid sparse/dense, structure. In this paper, we study the application to UWA channels of a novel *Hybrid Sparse/Diffuse* (HSD) model, originally proposed in [13] for Ultra-Wide Band (UWB) systems. This model combines both a *diffuse component*, to model the multipath

fading arising in dense multipath scenarios, and a *sparse component*, to model the fine-grained delay resolution at the receiver relative to the interarrival time of the resolvable multipath components. Moreover, we propose to use an exponential Power Delay Profile (PDP) for the diffuse component, and measure how this model fits the sample PDP measured from a representative subset of the SPACE08 data set. On the same data set, we then evaluate the Mean Squared Error (MSE) accuracy for the prediction of the observed sequence attained by HSD channel estimators; we compare our new estimators with conventional purely sparse and LS estimators.

We show that the assumption of an exponential PDP is accurate in shallow water environments where the receiver is far away from the transmitter, whereas a clustered model, according to which the channel is characterized by few strong, resolvable arrivals, each followed by a cluster of weaker arrivals, is more appropriate when the receiver is closer to the transmitter. Channel estimation strategies based on the HSD model and on the exponential PDP model for the diffuse component attain a better estimation accuracy than conventional LS based and purely sparse estimators, in scenarios where the exponential PDP model fits well the observed behavior of the diffuse component. Nevertheless, these estimators are found to be robust even in scenarios where the measured UWA channel does not exhibit an exponential PDP shape or a diffuse nature.

The paper is organized as follows. In Section II, we review the state of the art in UWA channel modeling, and we discuss the importance of employing a HSD model for the purpose of UWA channel estimation. In Section III, we present the system model and the HSD channel model. In Section IV, we design estimators specific to the HSD model, namely the *Generalized Thresholding* and the *Generalized MMSE* estimators. These estimators are evaluated on the SPACE08 experimental data set. Given that we assume an exponential PDP for the diffuse component, in Section V we show experimental results for the fitting of the exponential PDP model to the data. In Section VI, we provide numerical results and compare the prediction accuracy achieved by conventional purely sparse, LS estimators and the novel HSD estimators based on the exponential PDP model for the diffuse component. Finally, in Section VII we conclude the paper.

#### A. Notation

We use lower-case bold letters for column vectors ( $\mathbf{a}$ ), and upper-case bold letters for matrices ( $\mathbf{A}$ ). The scalar

$\mathbf{a}(k)$  denotes the  $k$ th entry of vector  $\mathbf{a}$ , and  $\mathbf{A}_{k,j}$  denotes the  $(k, j)$ th entry of matrix  $\mathbf{A}$ . The matrix  $\mathbf{A}^*$  is the transpose, complex conjugate of  $\mathbf{A}$ . The vector  $\mathbf{a} \odot \mathbf{b}$  is the component-wise (Schur) product of vectors  $\mathbf{a}$  and  $\mathbf{b}$ . The circular Gaussian distribution with mean  $\mathbf{m}$  and covariance  $\mathbf{\Sigma}$  is denoted by  $\mathcal{CN}(\mathbf{m}, \mathbf{\Sigma})$ . The Bernoulli distribution with parameter  $q$  is given by  $\mathcal{B}(q)$ . The indicator function is denoted by  $\mathcal{I}(\cdot)$ . The expectation of random variable  $x$ , conditioned on  $y$  is written as  $\mathbb{E}[x|y]$ .

## II. UNDERWATER ACOUSTIC CHANNEL MODELING

In this section, we review current channel models for UWA communications, and we present a novel Hybrid Sparse/Diffuse (HSD) model, originally proposed for UWB channels in [13]–[15]. This model, while retaining key physical features of the channel, lends itself to the design of estimators.

In the literature, we can broadly classify UWA channel modeling efforts into a *deterministic* approach and a *statistical* approach. The former aims to develop a static model, which is able to replicate the multipath arrival delays and amplitudes, once the environmental conditions are known. In this category, we include [16]–[18], which present studies of the physics involved in the interaction of sound waves with water conditions, the water bottom and surface. Of particular interest is the Bellhop tool [6], a ray-tracing algorithm which is able to predict the multipath arrival pattern of the channel, once the environmental conditions are known. The statistical approach tries to identify an accurate statistical model for the UWA channel, which can be used to develop and enhance signal processing techniques and algorithms for communications systems [5], [19]–[23]. In particular, these studies investigate the second order and complete statistics of the UWA channel impulse response in order to derive a suitable and realistic model for simulation studies and performance analysis.

While these models are important for realistic performance assessment, the full exploitation of the deterministic and statistical properties in the design of channel estimation techniques can be complex. For this reason, in this paper we seek a simplified channel model as a reference for the design of channel estimation strategies.

Due to the relatively slow propagation speed of sound waves in water ( $\sim 1.5$  km/s), propagation path length differences of only a few meters can result in delays of a few milliseconds between arrivals. With typical signal bandwidths on the order of 5 kHz in mid-frequency systems, such delays between arrivals are easily resolvable and can result in a sparse multipath structure.

However, in many scenarios of interest in UWA communications, *e.g.*, shallow water environments, a sparse channel structure is not sufficient to describe other UWA propagation mechanisms, *e.g.*, diffuse (dense) scattering, diffraction effects and frequency dispersion, which are better represented by a dense channel. We thus propose a novel HSD model, which views the channel as the superposition of two independent components: the sparse component, which models the resolvable multipath signals, owing to the fine delay resolution, and the diffuse component, which models other propagation phenomena that cannot be described by a sparse structure, such as dense scattering and frequency dispersion of UWA channels.

The HSD channel model is presented in detail in the following section.

### III. SYSTEM MODEL

We consider a point-to-point Underwater Acoustic channel. The source transmits a sequence of  $M$  pilot symbols,  $x(n), n = -(L-1), \dots, M-L$ , over a channel  $h(l), l = 0, \dots, L-1$  with known delay spread  $L \geq 1$ . The received discrete-time, baseband signal over the corresponding observation interval of length  $N = M - L + 1$ , is given by

$$y(n) = \sum_{l=0}^{L-1} h(l)x(n-l) + w(n), \quad n = 0, \dots, N-1,$$

where  $w(n) \in \mathcal{CN}(0, \sigma_w^2)$  is iid circular Gaussian noise. By collecting the  $N$  received, noise and channel samples in the column vectors  $\mathbf{y} = [y(0), y(1), \dots, y(N-1)]^T$ ,  $\mathbf{w} = [w(0), w(1), \dots, w(N-1)]^T \in \mathbb{C}^N$  and  $\mathbf{h} = [h(0), h(1), \dots, h(L-1)]^T \in \mathbb{C}^L$ , respectively, and letting  $\mathbf{X} \in \mathbb{C}^{N \times L}$  be the  $N \times L$  Toeplitz matrix associated with the pilot sequence, with the vector of the transmitted pilot sequence  $[x(-i), x(1-i), \dots, x(N-1-i)]^T$  as its  $i$ th column,  $i = 0, \dots, L-1$ , we have the following matrix representation:

$$\mathbf{y} = \mathbf{X}\mathbf{h} + \mathbf{w}. \quad (1)$$

The discrete baseband channel vector  $\mathbf{h}$  is modeled according to the HSD model developed in [13], [14] for UWB systems, *i.e.*,

$$\mathbf{h} = \mathbf{a}_s \odot \mathbf{c}_s + \mathbf{h}_d, \quad (2)$$

where  $\mathbf{a}_s \odot \mathbf{c}_s$  is the *sparse component*, and  $\mathbf{h}_d$  is the *diffuse component*. In particular,  $\mathbf{a}_s \in \{0, 1\}^L$  is the *sparsity pattern*, whose entries are equal to one in the positions corresponding to the resolvable multipath

components, and zero otherwise; its entries are drawn iid from  $\mathcal{B}(q)$ , where  $q \ll 1$  so as to enforce sparsity. Notice that the smaller  $q$ , the sparser the sparse component  $\mathbf{a}_s \odot \mathbf{c}_s$  is expected to be. The *sparse coefficient* vector  $\mathbf{c}_s$  is modeled as a deterministic and unknown vector. Finally, we use the Rayleigh fading approximation for the diffuse component,  $\mathbf{h}_d \sim \mathcal{CN}(\mathbf{0}, \Lambda_d)$ , where  $\Lambda_d$  is diagonal, with diagonal entries given by the PDP  $\mathcal{P}_d(k), k = 0, \dots, L-1$ .

*Remark 1.* We assume that  $\mathbf{c}_s$  is a deterministic and unknown vector, because the statistics of the specular components, that vary according to the large scale fading, are usually difficult to estimate. On the other hand, the Rayleigh fading assumption for the diffuse component is consistent with the fact that it arises from the contribution of multiple paths in a single resolvable delay bin. Its amplitude and phase vary according to the small scale fading. Its PDP can be accurately estimated by averaging the fading over subsequent realizations of the fading process. This information may then be used to estimate the channel via the linear Minimum Mean Squared Error (MMSE) estimator [24], which improves the accuracy over LS.

Notice that the LS estimate is a sufficient statistic for the channel. Therefore, we will refer to the following sufficient observation model

$$\mathbf{h}_{LS} = (\mathbf{X}^* \mathbf{X})^{-1} \mathbf{X}^* \mathbf{y} = \mathbf{h} + \mathbf{n}, \quad (3)$$

where  $\mathbf{n} \sim \mathcal{CN}(\mathbf{0}, \sigma_w^2 (\mathbf{X}^* \mathbf{X})^{-1})$ . In the following, we let  $\sigma_{LS}^2(k) = \sigma_w^2 [(\mathbf{X}^* \mathbf{X})^{-1}]_{k,k}$ . This represents the variance of the noise on the  $k$ th sample of the LS estimate. Therefore, we have  $\mathbf{n}(k) \sim \mathcal{CN}(0, \sigma_{LS}^2(k))$ .

### IV. HYBRID SPARSE/DIFFUSE CHANNEL ESTIMATORS

In [13], [14] we developed a three-step channel estimator based on the HSD model presented in the previous section:

- 1) The sparse coefficient vector  $\mathbf{c}_s$  is estimated via LS, giving the estimate  $\hat{\mathbf{c}}_s = \mathbf{h}_{LS}$ .
- 2) The sparsity pattern  $\mathbf{a}_s$  is estimated via either MMSE or Maximum A Posteriori (MAP) [24], giving the estimate  $\hat{\mathbf{a}}_s$ .
- 3) The diffuse component  $\mathbf{h}_d$  is estimated via MMSE, based on the residual estimation error after removing the estimated sparse component,  $(\mathbf{1} - \hat{\mathbf{a}}_s) \odot \mathbf{h}_{LS}$ .

The overall estimate of the HSD channel is then given by

$$\hat{\mathbf{h}}(k) = \hat{\mathbf{a}}_s(k)\mathbf{h}_{LS} + (1 - \hat{\mathbf{a}}_s(k)) \frac{\hat{\mathcal{P}}_d(k)}{\hat{\mathcal{P}}_d(k) + \sigma_{LS}^2(k)} \mathbf{h}_{LS},$$

where  $\hat{\mathcal{P}}_d(k)$  is an estimate of  $\mathcal{P}_d(k)$ . We have two different estimators, depending on whether MAP or MMSE is used to estimate the sparsity pattern  $\mathbf{a}_s$ . Letting  $\alpha = \ln\left(\frac{1-\tilde{q}}{\tilde{q}}\right)$ , where  $\tilde{q} \in (0,1)$  is an algorithm parameter, the *Generalized MMSE* (G-MMSE) estimator computes a MMSE estimate of  $\mathbf{a}_s$ , given by

$$\hat{\mathbf{a}}_s^{MMSE}(k) = \frac{1}{1 + e^\alpha \exp\left\{-\frac{|\mathbf{h}_{LS}(k)|^2}{\hat{\mathcal{P}}_d(k) + \sigma_{LS}^2(k)}\right\}}. \quad (4)$$

On the other hand, the *Generalized Thresholding* (G-Thres) estimator computes a MAP estimate of  $\mathbf{a}_s$ , given by

$$\hat{\mathbf{a}}_s^{MAP}(k) = \mathcal{I}\left\{|\mathbf{h}_{LS}(k)|^2 > \alpha \left(\hat{\mathcal{P}}_d(k) + \sigma_{LS}^2(k)\right)\right\}. \quad (5)$$

This solution determines a thresholding of the LS estimate, hence the name. The intuitive idea behind the G-Thres estimator is that the LS samples sufficiently *above* the "noise" floor, represented by the sum of the strengths of the noise and diffuse components, are regarded as active sparse components, whose coefficients are estimated via LS, whereas the LS samples below this level are regarded as diffuse components and are estimated via MMSE. A similar intuition holds for the G-MMSE estimator.

The parameter  $q$  is the true Bernoulli parameter for  $\mathbf{a}_s$ , in contrast  $\tilde{q}$  is the value assumed for the estimation phase [14], [15], which might be different from the true parameter. Moreover, using  $\tilde{q} < q$  improves the MSE estimation accuracy over using the true  $q$ , in the asymptotic low and high Signal to Noise Ratio (SNR) regimes [15]. Knowledge of the parameter  $q$  is thus not crucial, since a conservative approach in the estimation of the sparse component usually improves the estimation accuracy.

## V. POWER DELAY PROFILE MODELING

In this section, we model the PDP of the diffuse component. In particular, we assume an exponential PDP, and we measure the fitting of this model to the sample PDP estimated from the data, based on the SPACE08 data set. For more details on this data set, we refer the interested reader to [25]. In particular, we consider two different receivers, S3 and S5, located at 200 m and

1000 m distance from the transmitter, respectively. The environment can be classified as shallow water, since the seabed is 15 m below the sea surface.

The source transmits a pseudo-noise sequence of length 60 s, with symbols drawn from  $\{-1,1\}$  at rate 6510 symbols/s. The corresponding received sequence is divided into sub-sequences of length 30 ms each, corresponding to  $N = 194$  samples. Let  $\mathbf{y}^{(i)}$  be the observation vector from the  $i$ th sub-sequence, and  $\mathbf{X}^{(i)}$  be the Toeplitz matrix associated with the corresponding pilot sequence. A time series of LS channel estimates with delay spread 15 ms ( $L = 97$  samples) is generated as  $\mathbf{h}_{LS}^{(i)} = (\mathbf{X}^{(i)*}\mathbf{X}^{(i)})^{-1}\mathbf{X}^{(i)*}\mathbf{y}^{(i)}$ . This time series therefore represents the samples of the time-varying channel spaced in time 30 ms apart.

The sample PDP is computed by averaging over  $N_{ch} = 1878$  subsequent channel realizations, corresponding to an observation window of 56 s. We have

$$\hat{\mathcal{P}}_{sample}(k) = \frac{1}{N_{ch}} \sum_{i=0}^{N_{ch}-1} \left| \mathbf{h}_{LS}^{(i)}(k) \right|^2. \quad (6)$$

We now evaluate the exponential model for the PDP of the diffuse component, and we compare it with the sample PDP estimated from the data. At this point, since we are not assuming any a priori model for the PDP, and therefore we cannot distinguish the specular components from the diffuse background, which is unknown, we keep the sparse component to compute the sample PDP and the exponential fitting.

Let  $\mathcal{P}_d(k) = \beta e^{-\omega k}$ ,  $k = 0, \dots, L-1$  be the exponential PDP as a function of the channel delay. This is parameterized by the *power*  $\beta$ , and the *decay*  $\omega$ . Notice that  $\ln \mathcal{P}_d(k) = \ln \beta - \omega k = \rho - \omega k$ , where we have defined  $\rho = \ln \beta$ . These parameters can be estimated by computing a linear fitting of  $\ln \hat{\mathcal{P}}_{sample}(k)$ , *i.e.*, by solving

$$\{\hat{\rho}, \hat{\omega}\} = \arg \min_{\rho, \omega} \sum_k \left| \ln \hat{\mathcal{P}}_{sample}(k) - \rho + \omega k \right|^2. \quad (7)$$

We then determine the fitting error of the estimated exponential PDP with the sample PDP estimate as

$$f\left(\hat{\mathcal{P}}_{sample}\right) = \sum_k \left| \ln \hat{\mathcal{P}}_{sample}(k) - \hat{\rho} + \hat{\omega} k \right|^2. \quad (8)$$

Figure 1 shows the fitting error for the two receivers S3 and S5, respectively, over a representative subset of the SPACE08 data set. We notice that S5, which is the receiver farther away from the transmitter, fits the exponential PDP better than receiver S3. This may be

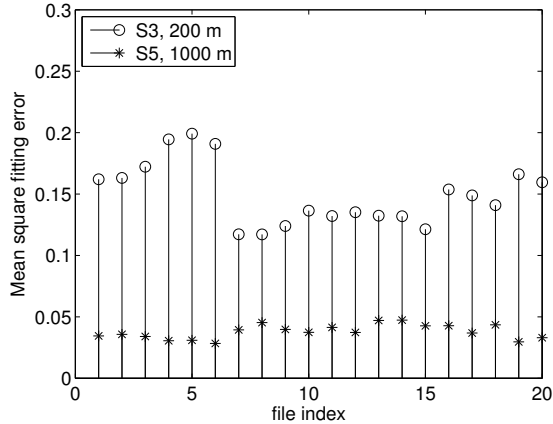


Figure 1: Fitting error of the sample PDP, estimated from the data, to the exponential PDP. The smaller the error, the better the fitting of the sample PDP to the exponential model.

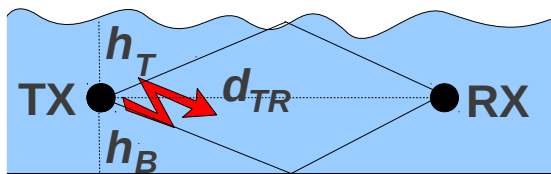
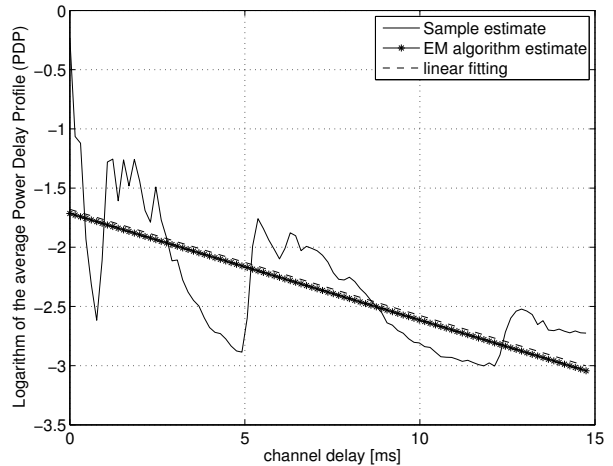


Figure 2: A shallow water scenario, with the line of sight component, and two echoes reflected by the seabed and the water surface.

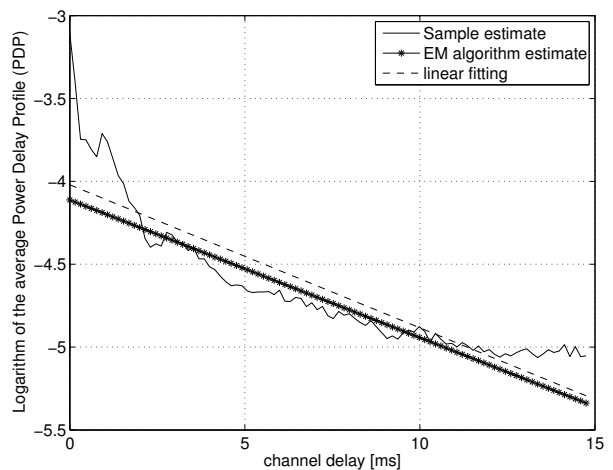
due to a multiplicative loss at each water surface or bottom bounce and an exponential absorption loss of the propagation medium.

Figure 3 shows a typical diffuse PDP for receivers S3 and S5, respectively. We observe that receiver S5 exhibits a more diffuse channel than receiver S3, and a good fitting to the exponential model. On the other hand, for receiver S3 a clustered model, where few strong resolvable multipath components are followed by a cluster of arrivals, seems more appropriate. This behavior can be interpreted with the help of Figure 2, which represents a shallow water scenario with the line of sight component and two echoes reflected by the seabed and the water surface, respectively.

Let  $d_{TR}$  be the distance between transmitter and receiver,  $h_T$  the depth of the transmitter/receiver pair below the sea level,  $h_B$  their height above the seabed, and  $c \simeq 1.5$  km/s the speed of the sound wave in the water. The line of sight component reaches the receiver with a delay  $\frac{d_{TR}}{c}$ . The echo reflected by the sea surface reaches the receiver with a delay  $\frac{\sqrt{d_{TR}^2 + 4h_T^2} + d_{TR}}{c}$ , ideally assuming



(a) Receiver S3



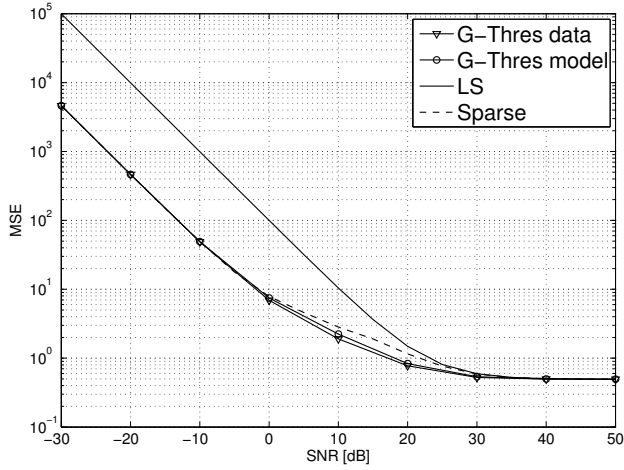
(b) Receiver S5

Figure 3: A typical sample PDP for receivers S3 and S5, with the exponential PDP estimated by linear fitting, and the PDP estimate based on the EM algorithm [14].

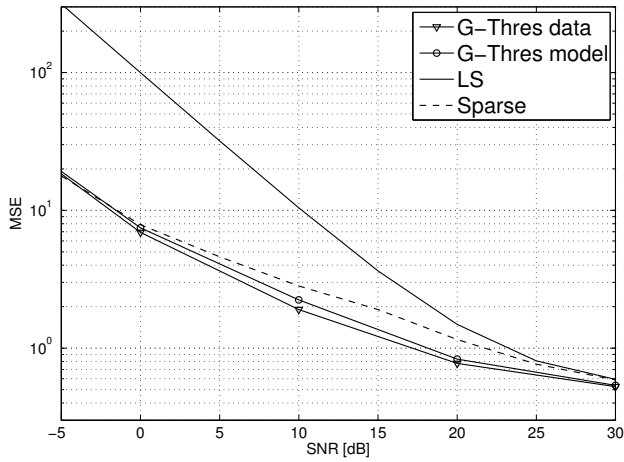
that the reflection occurs at distance  $\frac{d_{TR}}{2}$  from the source (a similar expression holds for the echo reflected by the seabed). Therefore, the interarrival time between the line of sight and the echo reflected by the sea surface is given by  $\tau_{inter}(d_{TR}) = \frac{\sqrt{d_{TR}^2 + 4h_T^2} - d_{TR}}{c}$ , which is a decreasing function of  $d_{TR}$ . Therefore, the further away the receiver from the transmitter, the smaller the interarrival time, the richer the interaction of the multipath components, and the more diffuse the nature exhibited by the UWA channel.

## VI. NUMERICAL RESULTS

We now present some numerical results, and we compare the mean squared prediction error of the received sequence using HSD, LS, and a purely sparse estimator,



(a) Entire SNR range



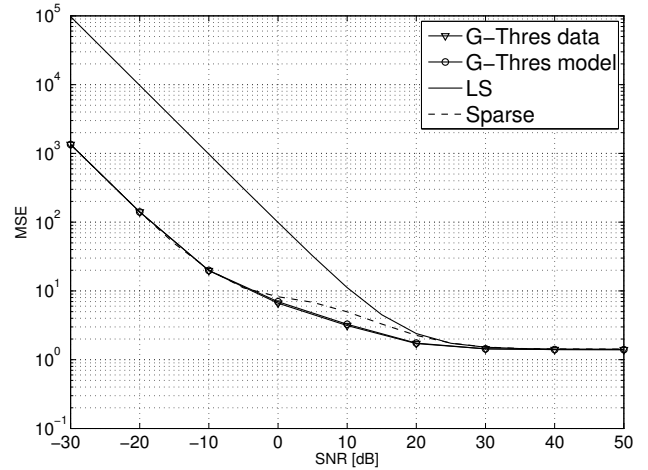
(b) Zoom in medium SNR range

Figure 4: Mean squared prediction error of the observed sequence for receiver S3, G-Thres estimator.

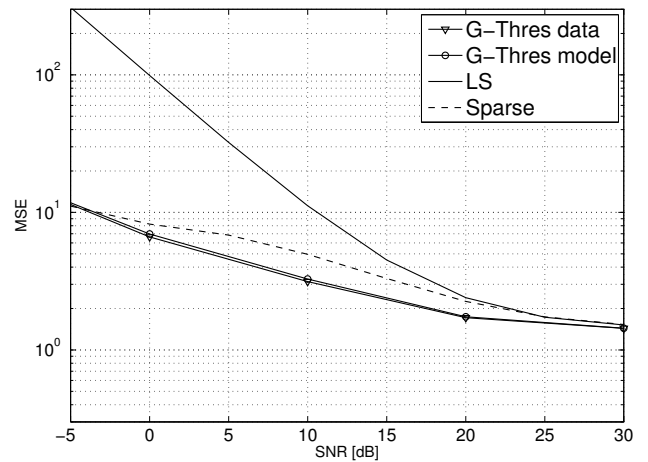
as a function of the SNR. In order to generate all the SNR values of interest, we add the UWA noise sequence  $\mathbf{w}^{(i)}$ , scaled by a factor  $\sqrt{S}^{-1} > 0$ , to the received sequence  $\mathbf{y}^{(i)}$  in the estimation phase, so as to induce SNR dependent channel estimation errors. Letting  $\hat{\mathbf{h}}^{(i)}$  be the  $i$ th channel estimate, estimated from the noisy received sequence  $\mathbf{y}^{(i)} + \sqrt{S}^{-1} \mathbf{w}^{(i)}$ ,  $\mathbf{y}^{(i+1)}$  be the observed sequence that we want to predict, and  $\mathbf{X}^{(i+1)}$  be the Toeplitz matrix associated with the corresponding pilot sequence, the MSE for the prediction of  $\mathbf{y}^{(i+1)}$  is defined as

$$\mathbb{E} \left[ \left\| \mathbf{y}^{(i+1)} - \mathbf{X}^{(i+1)} \hat{\mathbf{h}}^{(i)} \right\|_2^2 \right], \quad (9)$$

where the expectation is computed with respect to the realizations of the noise (intrinsic noise in the experimental data set and additional noise  $\mathbf{w}^{(i)}$ ) and of the



(a) Entire SNR range

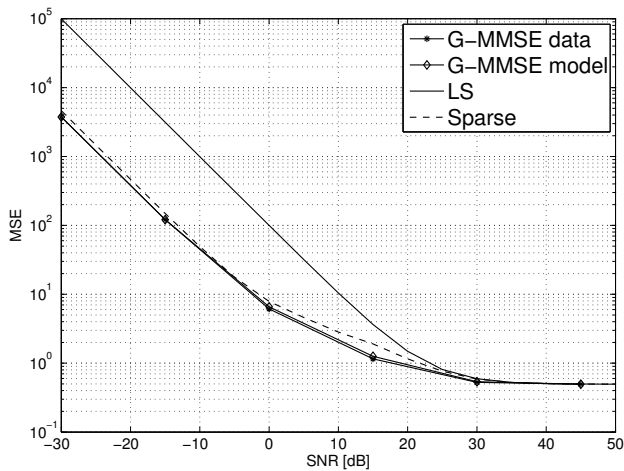


(b) Zoom in medium SNR range

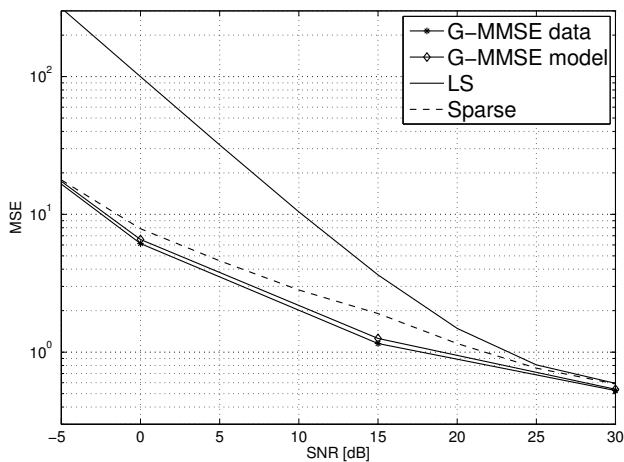
Figure 5: Mean squared prediction error of the observed sequence for receiver S5, G-Thres estimator.

channel. The overall mean squared prediction error is computed by averaging the sample squared error term  $\left\| \mathbf{y}^{(i+1)} - \mathbf{X}^{(i+1)} \hat{\mathbf{h}}^{(i)} \right\|_2^2$  over the sub-sequence index  $i$ , and over multiple received sequences, each 60s long, collected over different times and environmental conditions.

For the HSD model, we consider the G-Thres estimator, with  $\alpha = \ln \left( \frac{1-\tilde{q}}{\tilde{q}} \right)$ ,  $\tilde{q} = 0.001$ . For the sake of clarity of exposition, we provide the results for the G-Thres and G-MMSE estimators in separate figures. Moreover, we discuss the results only for the G-Thres estimator, since the same considerations hold for the G-MMSE estimator. We consider two different cases for the estimate of the PDP of the diffuse component: the sample PDP estimate, averaged over  $N_{ch} = 1878$  subse-

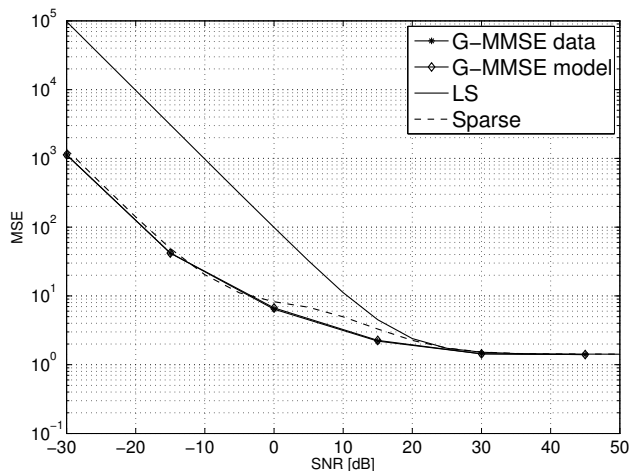


(a) Entire SNR range

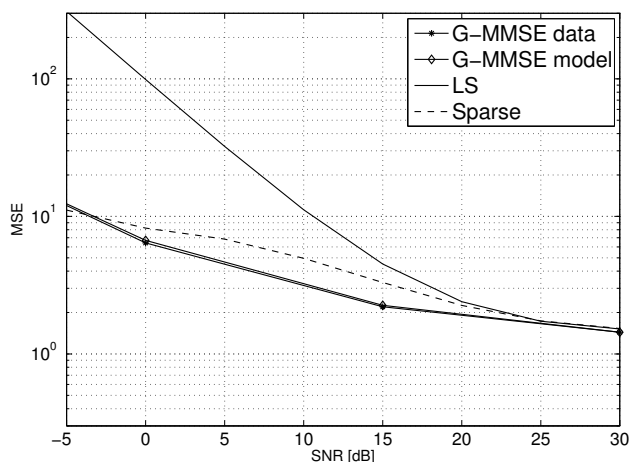


(b) Zoom in medium SNR range

Figure 6: Mean squared prediction error of the observed sequence for receiver S3, G-MMSE estimator.



(a) Entire SNR range



(b) Zoom in medium SNR range

Figure 7: Mean squared prediction error of the observed sequence for receiver S5, G-MMSE estimator.

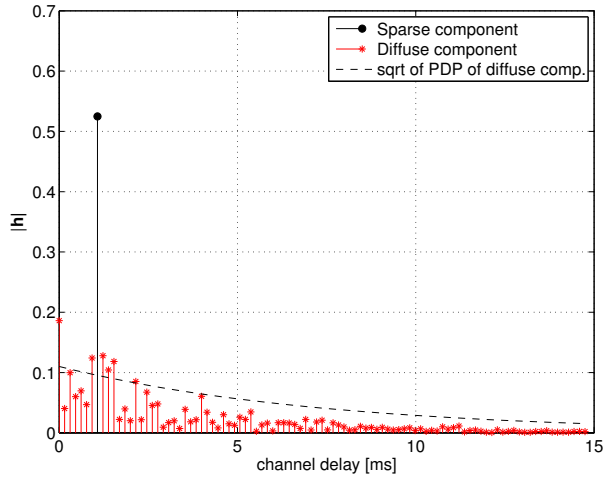
quent channel realizations, corresponding to a temporal window of 56 s; and the exponential PDP model, based on only one channel realization. In the latter case, we employ the Expectation-Maximization (EM) algorithm [26] developed in [14], which exploits the HSD structure of the channel to jointly estimate the sparse and diffuse components, and the power  $\beta$  and decay rate  $\omega$  of the exponential PDP of the diffuse component. One realization of the channel is sufficient in this case, due to the structure of the PDP which makes it possible to average the fading over the delay dimension, rather than over subsequent channel realizations.

As to the purely sparse case, we employ the G-Thres estimator assuming no diffuse component, to allow a fair comparison with the HSD model. This estimator, due to its thresholding operation, generates a sparse channel

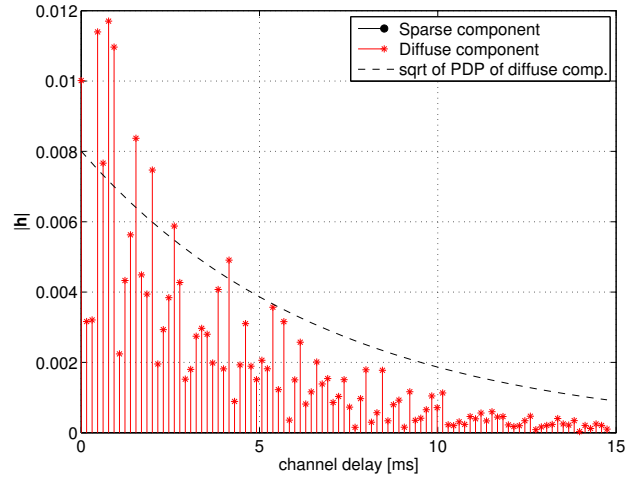
structure.

Figures 4 and 5 show the mean squared prediction error for receivers S3 and S5 for the G-Thres estimator, respectively. In particular, the labels "G-Thres data" and "G-Thres model" refer to the G-Thres estimators using the sample estimate of the PDP of the diffuse component and the exponential PDP model, respectively.

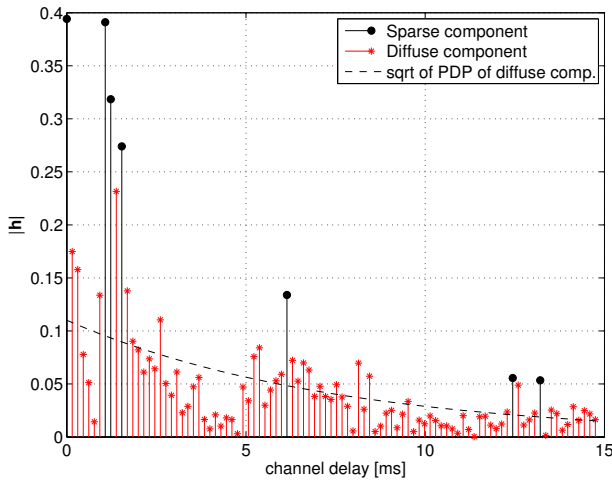
We notice that both the G-Thres and the sparse estimators perform better than LS, as observed in [7], [8], [11] for other sparse estimators. Moreover, in the low SNR region the G-Thres and the purely sparse estimators achieve the same prediction error. In fact, in this region, the diffuse component  $\mathbf{h}_d$  is below the noise floor, and cannot thus be distinguished from the noise. Therefore, an accurate estimate of  $\mathbf{h}_d$  is not possible in this regime, and the HSD model does not bring any advantage over



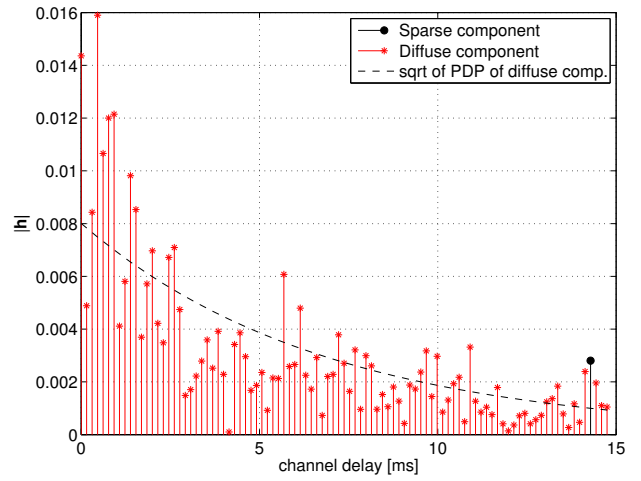
(a) SNR=10dB



(a) SNR=10dB



(b) SNR=50dB



(b) SNR=50dB

Figure 8: G-Thres estimator, estimated sparse and diffuse components for receiver S3.

Figure 9: G-Thres estimator, estimated sparse and diffuse components for receiver S5.

a purely sparse one. On the other hand, in the high SNR region all the estimators converge to the prediction error of LS. This can be explained with the fact that, when the noise level is negligible compared to the signal level, the prior knowledge about the channel structure provides no useful information. Moreover, the prediction error floor for high SNR is the result of intrinsic noise in the experimental data set, and of channel perturbations over subsequent observation intervals (notice that the prediction error floor is different for receivers S3 and S5, due to the fact that they incur different noise levels and rate of channel variations).

The G-Thres estimators outperform the purely sparse estimator in the medium SNR range. In fact, although based on a simplified model of the diffuse and the sparse

components, they are able to capture further diffuse structure of the UWA channel, which is discarded by a purely sparse estimator.

Comparing the two G-Thres estimators (with sample PDP estimate of the diffuse component and exponential PDP model), we observe that the best prediction accuracy is achieved by the G-Thres estimator with the sample estimate of the PDP. However, the G-Thres estimator based on the exponential model for the PDP performs very close to this lower bound, although some performance loss can be observed in the medium SNR range, due to a non perfect fitting of the data to the model.

Notice that a similar behavior of the estimators can be observed for receivers S3 and S5, despite the fact

that receiver S3 exhibits a sparser channel structure than receiver S5. We conclude that the G-Thres estimator is robust, and achieves good estimation accuracy even in channels which do not exhibit a diffuse nature.

Similar considerations hold for the G-MMSE estimator, whose prediction error is shown in Figures 6 and 7 for receivers S3 and S5, respectively.

Finally, in Figures 8 and 9 we plot the outputs of the G-Thres estimator, with the estimate of the sparse and diffuse components, for a channel realization at receivers S3 and S5, respectively, and for the high and medium SNR regimes. We notice that only one specular component is detected at receiver S5 at high SNR. In fact, receiver S5 exhibits a more diffuse channel, and a good fitting to the exponential PDP model, as discussed in Section V. On the other hand, a larger number of sparse components are detected at receiver S3, which exhibits a sparser structure (Figure 3). Also, we observe that fewer sparse components are detected at medium SNR, than at high SNR. In fact, the threshold level decreases with the SNR (see equation (5)), and thus fewer specular components can be distinguished from the noise and diffuse background as the SNR decreases.

## VII. CONCLUDING REMARKS

In this paper, we have proposed the use of a Hybrid Sparse/Diffuse (HSD) model for Underwater Acoustic channels. This model is appropriate in scenarios where the channel exhibits a dense arrival of multipath components, *e.g.*, in shallow water environments. Moreover, based on previous work [13]–[15] for Ultra Wideband systems, we have proposed estimation strategies based on the HSD channel model, namely the *Generalized MMSE* and the *Generalized Thresholding* estimators.

We have tested the exponential power delay profile for the diffuse component in the SPACE08 data set, and verified that this model fits well in scenarios where the receiver is far from the transmitter and the environmental scattering gives rise to multipath fading. We have shown by numerical results that the HSD estimators outperform purely sparse and least squares estimators in the medium SNR regime. Moreover, the HSD estimators based on the exponential model for the PDP of the diffuse component are robust, and achieve high accuracy even in scenarios where the receiver exhibits a clustered channel structure.

## ACKNOWLEDGMENT

This research has been funded in part by the following grants and organizations: ONR N00014-09-1-0700, NSF CNS-0832186, NSF CNS-0821750 (MRI), ONR N00014-05-10085, ONR N00014-10-10422, by the

European Commission under the Seventh Framework Programme (Grant Agreement 258359 – CLAM) and by the Aldo Gini Foundation (Padova, Italy).

## REFERENCES

- [1] I. F. Akyildiz, D. Pompili, and T. Melodia, "State-of-the-art in protocol research for underwater acoustic sensor networks," in *Proceedings of the 1st ACM international workshop on Underwater networks*, New York, NY, USA, 2006, pp. 7–16.
- [2] J. Heidemann, W. Ye, J. Wills, A. Syed, and Y. Li, "Research challenges and applications for underwater sensor networking," in *IEEE Wireless Communications and Networking Conference*, vol. 1, Apr. 2006, pp. 228–235.
- [3] T. Eggen, A. Baggeroer, and J. Preisig, "Communication over Doppler spread channels. Part I: Channel and receiver presentation," *IEEE Journal of Oceanic Engineering*, vol. 25, no. 1, pp. 62–71, Jan. 2000.
- [4] T. Eggen, J. Preisig, and A. Baggeroer, "Communication over Doppler spread channels. Part II: Receiver characterization and practical results," *IEEE Journal of Oceanic Engineering*, vol. 26, no. 4, pp. 612–621, Oct. 2001.
- [5] M. Stojanovic and J. Preisig, "Underwater acoustic communication channels: Propagation models and statistical characterization," *IEEE Communications Magazine*, vol. 47, no. 1, pp. 84–89, Jan. 2009.
- [6] M. Porter *et al.*, "Bellhop code." [Online]. Available: <http://oalib.hlsresearch.com/Rays/index.html>
- [7] C. Berger, S. Zhou, J. Preisig, and P. Willett, "Sparse channel estimation for multicarrier underwater acoustic communication: From subspace methods to compressed sensing," *IEEE Transactions on Signal Processing*, vol. 58, no. 3, pp. 1708–1721, Mar. 2010.
- [8] C. Carbonelli, S. Vedantam, and U. Mitra, "Sparse channel estimation with zero tap detection," *IEEE Transactions on Wireless Communications*, vol. 6, no. 5, pp. 1743–1763, May 2007.
- [9] A. S. Gupta and J. Preisig, "An adaptive sparse sensing approach to shallow water acoustic channel estimation and tracking," *The Journal of the Acoustical Society of America*, vol. 128, no. 4, pp. 2354–2354, 2010.
- [10] N. Richard and U. Mitra, "Sparse channel estimation for cooperative underwater communications: A structured multichannel approach," in *IEEE International Conference on Acoustics, Speech and Signal Processing (ICASSP)*, Apr. 2008, pp. 5300–5303.
- [11] C. Pelekaniakis and M. Chitre, "Comparison of sparse adaptive filters for underwater acoustic channel equalization/estimation," in *International Conference on Communication Systems (ICCS)*, Nov. 2010, pp. 395–399.
- [12] P. Van Walree, "Channel sounding for acoustic communications: techniques and shallow-water examples," Norwegian Defence Research Establishment (FFI), Tech. Rep. FFI-rapport 2011/00007, Apr. 2011. [Online]. Available: [rapporter.ffi.no/rapporter/2011/00007.pdf](http://rapporter.ffi.no/rapporter/2011/00007.pdf)
- [13] N. Michelusi, U. Mitra, and M. Zorzi, "Hybrid Sparse/Diffuse UWB Channel Estimation," in *2011 IEEE 12th International Workshop on Signal Processing Advances in Wireless Communications (SPAWC 2011)*, San Francisco, USA, June 2011.
- [14] N. Michelusi, U. Mitra, A. Molisch, and M. Zorzi, "UWB Sparse/Diffuse Channels, Part I: Channel Models and Bayesian Estimators," 2011, submitted to *IEEE Transactions on Signal Processing*.

- [15] —, “UWB Sparse/Diffuse Channels, Part II: Estimator Analysis and Practical Channels,” 2011, submitted to *IEEE Transactions on Signal Processing*.
- [16] F. Jensen, W. Kuperman, M. Porter, and H. Schmidt, *Computational Ocean Acoustics*, 2nd ed. New York: Springer-Verlag, 2011.
- [17] R. Urick, *Principles of Underwater Sound*. McGraw-Hill, 1983.
- [18] L. Brekhovskikh and Y. Lysanov, *Fundamentals of ocean acoustics*, 3rd ed. New York: Springer-Verlag, 2003.
- [19] T. C. Yang, “Measurements of temporal coherence of sound transmissions through shallow water,” *Journal of the Acoustic Society of America*, vol. 120, no. 5, pp. 2595–2614, Nov. 2006.
- [20] —, “Temporal coherence of sound transmissions in deep water revisited,” *Journal of the Acoustic Society of America*, vol. 124, no. 1, pp. 113–127, July 2008.
- [21] A. G. Zajic, “Statistical space-time-frequency characterization of MIMO shallow water acoustic channels,” in *Proc. of IEEE OCEANS*, Biloxi, Oct. 2009.
- [22] P. Qarabaqi and M. Stojanovic, “Statistical Modeling of a Shallow Water Acoustic Communication Channel,” in *Proc. Underwater Acoustic Measurements Conference (UAM)*, Jun. 2009.
- [23] J. Zhang, J. Cross, and Y. Zheng, “Statistical channel modeling of wireless shallow water acoustic communications from experiment data,” in *Military Communications Conference (MILCOM)*, Nov. 2010.
- [24] E. L. Lehmann and G. Casella, *Theory of Point Estimation*, 2nd ed. Springer, Aug. 1998.
- [25] B. Tomasi, J. Presig, G. Deane, and M. Zorzi, “A Study on the Wide-Sense Stationarity of the Underwater Acoustic Channel for Non-coherent Communication Systems,” in *European Wireless Conference*, Apr. 2011.
- [26] A. P. Dempster, N. M. Laird, and D. B. Rubin, “Maximum likelihood from incomplete data via the EM algorithm,” *Journal of the Royal Statistical Society, B*, vol. 39, 1977.